The Astrophysical Journal Letters, 867:L10 (6pp), 2018 November 1 https://doi.org/10.3847/2041-8213/aae7cb

A Search for the Host Galaxy of FRB 171020

Elizabeth K. Mahony[1], Ron D. Ekers[1], Jean-Pierre Macquart[2], Elaine M. Sadler[1,3], Keith W. Bannister[1], Shivani Bhandari[1], Chris Flynn[4], Bärbel S. Koribalski[1], J. Xavier Prochaska[5,6], Stuart D. Ryder[7], Ryan M. Shannon[4], Nicolas Tejos[8], Matthew T. Whiting[1], and O. I. Wong[9]
[1] Australia Telescope National Facility, CSIRO Astronomy and Space Science, PO Box 76, Epping NSW 1710, Australia; elizabeth.mahony@csiro.au
[2] International Centre for Radio Astronomy Research, Curtin University, Bentley WA 6102, Australia
[3] Sydney Institute for Astronomy, School of Physics A28, The University of Sydney, NSW 2006, Australia
[4] Centre for Astrophysics and Supercomputing, Swinburne University of Technology, John Street, Hawthorn VIC 3122, Australia
[5] University of California, Santa Cruz, 1156 High Street, Santa Cruz, CA 95064, USA
[6] Kavli Institute for the Physics and Mathematics of the Universe (Kavli IPMU), 5-1-5 Kashiwanoha, Kashiwa, 277-8583, Japan
[7] Department of Physics and Astronomy, Macquarie University, NSW 2109, Australia
[8] Instituto de Física, Pontificia Universidad Católica de Valparaíso, Casilla 4059, Valparaíso, Chile
[9] International Centre for Radio Astronomy Research-M468, The University of Western Australia, 35 Stirling Highway, Crawley WA 6009, Australia
Received 2018 September 20; revised 2018 October 8; accepted 2018 October 11; published 2018 October 29

Abstract

We report on a search for the host galaxy of FRB 171020, the fast radio burst (FRB) with the smallest recorded dispersion measure (DM; DM = 114 pc cm^{-3}) of our ongoing ASKAP survey. The low DM confines the burst location within a sufficiently small volume to rigorously constrain the identity of the host galaxy. We identify 16 candidate galaxies in the search volume and single out ESO 601–G036, an Sc galaxy at redshift $z = 0.00867$, as the most likely host galaxy. Ultraviolet and optical imaging and spectroscopy reveal that this galaxy has a star formation rate of approximately 0.1 $M_{\odot}$ yr^{-1} and oxygen abundance $12 + \log(\mathrm{O/H}) = 8.3 \pm 0.2$, properties that are remarkably consistent with the galaxy hosting the repeating FRB 121102. However, in contrast to FRB 121102, follow-up radio observations of ESO 601–G036 show no compact radio emission above a 5σ limit of $L_{2.1\mathrm{GHz}} = 3.6 \times 10^{19}$ W Hz^{-1}. Using radio continuum observations of the field, combined with archival optical imaging data, we find no analog to the persistent radio source associated with FRB 121102 within the localization region of FRB 171020 out to $z = 0.06$. These results suggest that FRBs are not necessarily associated with a luminous and compact radio continuum source.

Key words: galaxies: individual (ESO 601–G036) – galaxies: spiral – radio continuum: galaxies

1. Introduction

The progenitors and local environments responsible for the bright ($F_{\nu} \sim 0.55$–380 Jy ms; Petroff et al. 2016), extragalactic millisecond-duration pulses known as fast radio bursts (FRBs) are open questions. Only a single known repeating FRB (121102; Spitler et al. 2016) has been localized with sufficient accuracy to unambiguously identify its host galaxy (Chatterjee et al. 2017; Tendulkar et al. 2017) and permit examination of the burst environment. Its host galaxy, a low-metallicity dwarf galaxy at redshift $z = 0.193$, harbors a "persistent" compact radio source (Chatterjee et al. 2017) co-located within 40 pc of the FRB (Marcote et al. 2017). The radio source, and therefore the FRB, likely resides in a bright star-forming region in the outskirts of the galaxy (Bassa et al. 2017). The persistent radio source has inspired suggestions that detections of bright radio emission may help to identify hosts of other FRBs (Eftekhari et al. 2018).

However, the unusual properties of FRB 121102 make it difficult to apply these findings to other FRBs. So far, no other FRBs have been observed to repeat, despite extensive follow-up campaigns (e.g., Bhandari et al. 2018). Radio diagnostics of the repeater's host galaxy and circumburst medium reveal that FRB 121102 resides in a highly magnetized medium (Michilli et al. 2018) whose rotation measure exceeds other FRB measurements by 3–4 orders of magnitude (Masui et al. 2015; Petroff et al. 2017; Caleb et al. 2018).

Here we examine FRB 171020 which has the lowest dispersion measure (DM) measured to date (114 pc cm^{-3}; Shannon et al. 2018). No repeat bursts above a signal-to-noise ratio (S/N) of 9 were found in 32.7d of observations. Despite the large localization region of this FRB, 50 × 34 arcmin at a position angle of 29°.6 (95% containment), its low DM demands a sufficiently close proximity to attempt identification of its host galaxy.

In Section 2 we report the properties of FRB 171020 and estimate the maximum redshift, followed by a search for its host galaxy in existing catalogs (Section 3). We discuss follow-up optical and radio observations of our best candidate host galaxy ESO 601–G036 in Section 4, and compare the properties of this galaxy with the host galaxy of FRB 121102 in Section 5, before concluding in Section 6. The cosmological parameters assumed in this Letter are from the Planck 2015 results (Planck Collaboration et al. 2016).

2. The Maximum Redshift of FRB 171020

We use the DM of FRB 171020 to estimate an upper limit to its distance. We assume that the total DM is given by

$$\mathrm{DM} = \mathrm{DM_{MW(disk)}} + \mathrm{DM_{MW(halo)}} + \mathrm{DM_{IGM}} + \mathrm{DM_{Host}}$$

where $\mathrm{DM_{MW(disk)}}$ and $\mathrm{DM_{MW(halo)}}$ are the contributions, respectively, of the Milky Way disk interstellar medium (ISM) and halo, $\mathrm{DM_{IGM}}$ is the contribution of the intergalactic medium along the line of sight, and $\mathrm{DM_{Host}}$ is the contribution from both the host galaxy itself and its circumburst environment. Given that the DM of FRB 171020 is so low, the contribution from the Milky Way represents a significant fraction of the total. As such, the assumptions used to derive

Table 1
Estimates for the DM Contributions (in pc cm^{-3}) from the Milky Way (MW) and FRB Host Galaxy, as Described in Section 2 of the Text

	YMW16		NE2001	
Model	**(a)**	**(b)**	**(c)**	**(d)**
$DM_{total,\ obs}$	114	114	114	114
$DM_{MW(disk)}$	26	26	38	38
$DM_{MW(halo)}$	12	12	12	12
DM_{Host}	0	45	0	45
DM_{IGM}	76	31	64	19
z_{est}	0.08	0.03	0.06	0.02

Note. The final row gives the estimated upper limit on the host galaxy redshift.

these quantities can lead to large fractional uncertainty in the maximum redshift of the FRB.

At the Galactic coordinates $(l,\ b) = (36.4, -53.6)$ of the burst, $DM_{MW(disk)}$ is 38 pc cm^{-3} according to the NE2001 model (Cordes & Lazio 2002), or 26 pc cm^{-3} following the YMW16 model (Yao et al. 2017).

The Milky Way halo contribution is much more uncertain; we assume $DM_{MW(halo)} = 12$ pc cm^{-3} calculated by using the excess DM of pulsars detected on the near side of the Large Magellanic Cloud (LMC; Manchester et al. 2005). By selecting the closest LMC pulsars it is assumed that there is negligible DM contribution from the LMC itself, and subtracting the Milky Way contribution leads to a halo contribution of $8 < DM_{MW(halo)} < 13$ pc cm^{-3} out to 50 kpc. Extragalactic FRBs travel farther, however, implying a higher $DM_{MW(halo)}$ that depends on its electron density distribution. Physically plausible models predict $DM_{MW(halo)}$ with an additional 2–21 pc cm^{-3} at distances >50 kpc (e.g., Miller & Bregman 2013, J. X. Prochaska & Y. Zheng, 2018, in preparation). This is consistent with the estimate of $DM_{MW(halo)} = 30$ pc cm^{-3} (Dolag et al. 2015), but we use a lower estimate here to determine the maximum redshift.

For DM_{Host}, we adopt two different assumptions. One assumes $DM_{Host} = 0$ pc cm^{-3}, and the other assumes $DM_{Host} = 45$ pc cm^{-3} typical for a dwarf galaxy (Xu & Han 2015). Note that DM_{Host} includes the halo, disk, and circumburst environment components of the host galaxy.

The two assumptions imply a range for DM_{IGM} of 0–76 pc cm^{-3} (Table 1). Adopting the relation between redshift and DM_{IGM} of $z \approx DM_{IGM}/1000$ (Ioka 2003; Inoue 2004) yields an upper limit on the redshift of $0.02 \lesssim z_{max} \lesssim 0.08$. Given the low observed DM of FRB 171020, the contribution from the intergalactic medium (IGM) could vary significantly depending on the number and properties of intervening galaxy halos (McQuinn 2014). However, given that the maximum redshift of $z = 0.08$ assumes conservative estimates of both the Milky Way halo and host galaxy contributions, any scatter in the DM-z relation is compensated for by the large range in maximum redshifts obtained by using the different models in Table 1.

3. Candidate Host Galaxies of FRB 171020

The area of the localization region of FRB 171020 (0.38 deg^2) and its maximum distance of 350 Mpc (using $z_{max} = 0.08$ from Model (a) in Table 1) together confine its host galaxy to a maximum comoving volume of 1620 Mpc^3. Taking the lower value of $z_{max} = 0.03$ from Model (b), the search volume is only 90 Mpc^3. These volumes are small enough to search for an optical host galaxy counterpart to FRB 171020 in spite of its poor localization. We searched the NASA Extragalactic Database for cataloged galaxies within the FRB localization ellipse, yielding only two galaxies with a published redshift at $z < 0.08$.

3.1. ESO 601–G036

ESO 601–G036 is a $B_J = 15.6$ Sc galaxy (Lauberts 1982) at a redshift of $z = 0.00867$ measured from H I emission detected in the H I Parkes All Sky Survey (HIPASS; Meyer et al. 2004). da Costa et al. (1998) listed an optical radial velocity of 2539 km s^{-1} ($z = 0.0085$), giving a distance of 37 Mpc using the the Mould et al. (2000) model. The absolute magnitude is $M_R = -17.9$, calculated from the SuperCOSMOS R-band after correcting for Galactic extinction.

The probability that ESO 601–G036 is a chance association may be estimated from the surface density of nearby galaxies. The Compact Binary Coalescence Galaxy (CBCG) catalog (Kopparapu et al. 2008) lists all star-forming galaxies to $z \sim 0.025$, including ESO 601–G036. The 0.38 deg^2 localization region for FRB 171020 gives a ~40% chance of finding a CBCG galaxy within the 2σ ellipse decreasing to a 10% probability if located in the 1σ localization area.

To expand this analysis out to higher redshifts we follow the method described in Eftekhari & Berger (2017) to calculate the probability that ESO 601–G036 is associated with FRB 171020. The large localization region yields a probability of a chance coincidence to be 1, meaning that ESO 601–G036 is far from a statistically robust identification beyond $z \sim 0.025$. In the following sections we search for other possible counterparts within the search volume.

3.2. 2MASX J22150112-1925373

This is an elliptical galaxy at $z = 0.0667$ (Jones et al. 2004) and absolute magnitude calculated from the SuperCOSMOS R-band magnitude of $M_R = -21.5$. At this redshift, the average DM_{IGM} implies $DM_{host} < 10$ pc cm^{-3}, which is implausible for this massive elliptical (Xu & Han 2015; Walker et al. 2018). This inconsistency and its location at the edge of the 95% confidence region make 2MASX J22150112 −1925373 an unlikely host of FRB 171020.

3.3. Candidates from the WISE × SCOSPZ Catalog

Existing redshift catalogs are incomplete for low-luminosity galaxies, so we expanded our search by using the WISE × SuperCOSMOS Photometric Redshift Catalog (WISE × SCOSPZ; Bilicki et al. 2016). The catalog magnitude limit includes LMC-like galaxies ($M_R = -18.5$) out to $z \sim 0.08$, but is incomplete to dwarfs beyond $z \sim 0.03$.

We found 16 objects with photometric redshifts $z_{ph} < 0.08$ within the localization region of FRB 171020, including ESO 601–G036. The other 15 objects all have photometric redshifts above $z = 0.04$, and are listed in Table 2. We conducted follow-up observations of five of these candidates with the X-Shooter spectrograph (Vernet et al. 2011) mounted on UT2 (Kueyen) of the European Southern Observatory's Very Large Telescope on 2018 Aug 3 UT. Each source was observed at two nod positions for a total on-source integration time of 360 s, through slit widths of 0.″9 in the near-infrared

Table 2
List of all Candidate Host Galaxies within the FRB 171020 Error Ellipse

#	Name	Prob.[a]	$S_{2.1\mathrm{GHz}}$ (mJy)	W1 (mag)	W2 (mag)	B (mag)	R (mag)	z	M_R (mag)	Notes
NASA/IPAC Extragalactic Database matches out to $z = 0.08$										
1	ESO 601−G036‡	1	0.3	14.7	14.6	15.0	15.0	0.00867	−17.9	
2	2MASX J22150112 −1925373‡	0.24	0.66	12.6	12.5	14.3	15.8	0.0667	−21.5	
WISE × SCOSPZ matches out to $z = 0.08$										
1	J221524.61−193504.8	1	0.3	14.7	14.6	15.0	15.0	0.00867	−17.9	ESO 601−G036
3	J221621.59−191829.9‡	0.23	<0.08	15.0	15.0	17.5	17.0	0.024	−18.2	
4	J221548.31−192225.0‡	0.34	<0.07	16.6	16.2	18.8	18.1	0.043†	−18.4	
5	J221601.96−193251.4‡	0.48	<0.09	15.7	15.5	17.8	17.6	0.055†	−19.4	
6	J221638.72−192651.0	0.54	<0.21	14.1	14.0	17.1	16.5	0.055†	−20.5	
7	J221413.69−194032.1‡	0.19	<0.24	16.6	16.5	19.0	18.3	0.056†	−18.8	
8	J221445.43−194502.2‡	0.57	<0.09	16.4	15.9	18.3	18.4	0.056†	−18.7	
9	J221649.58−192707.1	0.26	<0.26	16.5	16.1	18.8	18.2	0.057†	−18.9	
10	J221437.97−192453.2	0.13	<0.27	16.5	15.9	18.7	17.9	0.068†	−19.6	
11	J221611.23−191443.8	0.18	<0.27	16.0	15.8	18.5	17.8	0.066†	−19.7	
12	J221559.40−192629.3	0.53	<0.09	14.1	14.1	17.3	16.2	0.070†	−21.3	
13	J221449.49−192207.4	0.04	<0.21	16.0	15.6	18.2	18.1	0.071†	−19.5	
14	J221528.16−193851.9	0.85	<0.08	16.2	16.2	18.7	18.5	0.076†	−19.3	
15	J221503.26−192544.4	0.24	<0.21	14.2	14.1	17.4	16.8	0.079†	−21.1	
16	J221612.70−192222.1	0.52	<0.12	15.6	15.5	18.4	17.5	0.076†	−20.3	
17	J221618.08−194206.2	0.09	<0.18	14.3	14.0	17.3	16.9	0.079†	−20.9	
Possible FRB 121102 analogs: $S_{2.1\mathrm{GHz}} > 2.5$ mJy with optical counterparts in SuperCOSMOS										
18	J221430−195511	0.26	6.6	14.5	14.2	21.0	19.6	⋯	⋯	Luminous infrared galaxy (LIRG) WISE colors
19	J221507−194713‡	0.35	2.6	15.2	15.2	21.1	19.3	>0.1	⋯	
20	J221510−194835	0.35	2.8	15.2	15.0	19.6	18.6	0.17†	−21.1	
21	J221525−194518	0.62	5.4	16.4	15.7	21.1	20.2	⋯	⋯	Seyfert WISE colors
22	J221606−194032	0.26	4.0	15.5	14.1	20.1	19.2	⋯		Quasi-stellar object (QSO) WISE colors
23	J221612−194915‡	0.13	4.2	15.0	14.7	21.1	19.1	>0.1	⋯	
24	J221631−191942	0.30	3.2	14.2	13.9	20.1	18.1	0.35†	−23.3	

Note. Where available, optical and IR magnitudes are taken from the WISE × SCOSPZ catalog and have been extinction corrected; otherwise, magnitudes were obtained directly from the WISE and SuperCOSMOS databases (and not corrected for extinction). We report photometric redshifts from the WISE × SCOSPZ to 2 significant figures (denoted by †), but it is unlikely they are accurate to this level of significance. Source names marked by ‡ have been followed up spectroscopically with X-Shooter. A redshift was unable to be measured for six of these sources, indicating that they are outside of the search volume. The 2.1 GHz flux densities are measured from the deeper Australia Telescope Compact Array (ATCA) observations carried out on 2018 June 28. If undetected, 5 sigma limits measured at that position are listed.

[a] The probability density (scaled to the peak pixel) at that position in the localization region calculated by the detection of the FRB in multiple beams. See Bannister et al. (2017) for further details.

(NIR) and optical arms, and 1.″0 in the ultraviolet B (UVB) arm.

A spectroscopic redshift was obtained for only one of these targets: WISEJ221621.59−191829.9 at $z = 0.024$. While confirming that this object is at $z < 0.03$ makes it a more likely host galaxy candidate, it is also close to the edge of the 2σ error ellipse, which decreases the probability that it is the correct identification. No emission lines or significant stellar continuum were detected in either the UVB or optical spectra of the other four sources, indicating that they are most likely beyond our search volume.

4. Multi-wavelength Properties of ESO 601–G036

Given the low redshift and location close to the center of the localization ellipse, ESO 601–G036 is the most likely host galaxy of FRB 171020. In low-resolution images of this galaxy (i.e., DSS) there is a clear stellar tail just south of the galaxy (separately cataloged by Lauberts (1982) as ESO 601−G037). Bright UV emission of both objects, detected in *GALEX* images, indicates significant star formation that likely originated from tidal interactions or accretion of a dwarf galaxy companion. In the infrared, ESO 601–G036 is detected in the VISTA Hemisphere Survey with $Y = 14.53$, $J = 14.31$, $Ks = 13.73$ mag (Irwin et al. 2004). We estimate a total star formation rate (SFR) of $\sim 0.13\, M_\odot\, \mathrm{yr}^{-1}$ from the *GALEX* data,[10] and a total stellar mass of $\sim 9 \times 10^8\, \mathrm{M}_\odot$ from the VISTA *Ks*-band magnitude.

The HI Parkes All Sky Survey (HIPASS; Barnes et al. 2001) shows H I emission in ESO 601–G036, with an H I-integrated flux density of $\approx 7\ \mathrm{Jy\ km\ s^{-1}}$, corresponding to an H I mass of $2.3 \times 10^9\, M_\odot$.[11] For a rotational velocity of $\sim 80\ \mathrm{km\ s^{-1}}$ and maximum radius of 11 kpc, we derive a dynamical mass of $\sim 1.6 \times 10^{10}\, M_\odot$.

ESO 601–G036 is a member of a loose galaxy group, with four other gas-rich members detected in HIPASS at similar velocities. These other four galaxies lie outside the FRB 171020 2σ error region.

[10] This calculated SFR includes Galactic dust reddening and internal dust corrections as per Wong et al. (2016).

[11] These galaxy properties have been extracted from the HIPASS datacubes and differ slightly from those published by Meyer et al. (2004).

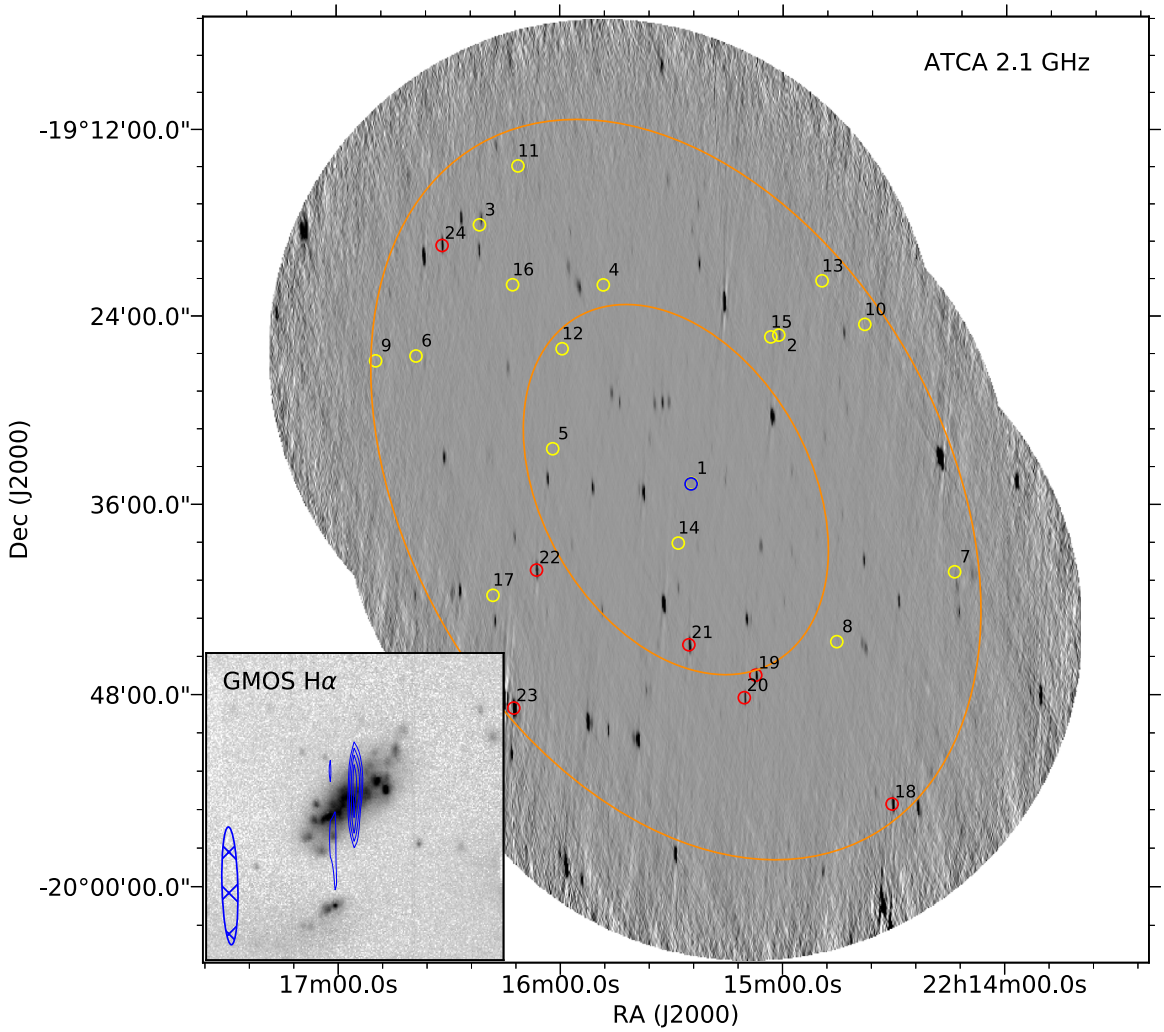

Figure 1. ATCA radio continuum image of the field of FRB 171020 at 2.1 GHz. The orange ellipses mark the 1σ and 2σ confidence localization regions of FRB 171020. Yellow circles are optically selected candidates from the WISE × SCOSPZ catalog listed in Table 2, red circles are radio-selected candidates (FRB 121102 analogs) discussed in Section 5.1. The blue circle highlights the position of ESO 601−G036. Inset: GMOS Hα image of the galaxy ESO 601–G036 overlaid with a deep ATCA 2.1 GHz radio continuum emission shown in blue contours. The contour levels are 0.08, 0.09, 0.1, and 0.11 mJy beam^{-1}. The ATCA synthesized beam ($37\farcs1 \times 5\farcs0$) is shown in the bottom-left corner. Candidate sources are labeled as in Table 2.

4.1. Optical Follow-up of ESO 601–G036

We observed ESO 601–G036 using the Gemini Multi-Object Spectrograph (GMOS; Hook et al. 2004; Gimeno et al. 2016) on Gemini-South on 2018 July 11 UT. We used the B600 grating with a $0\farcs75$ wide slit oriented along its major axis for a total of 5 minutes exposure time with wavelength coverage of 3700–6850 Å and dispersion of ≈1 Å/pixel.

The GMOS spectrum gives a redshift measurement of $z \approx 0.0082$, consistent with the H I observations. We observe strong Hα, [O III] emission lines but little [N II] emission, indicating that this is a low-metallicity galaxy. The flux ratios of $\log$ ([N II] $\lambda6583/$Hα) ≈ -1.09 and $\log\{$([O III] $\lambda5007/$Hβ)/([N II] $\lambda6583/$Hα)$\} \approx 1.41$ imply an oxygen abundance $12 + \log(\mathrm{O/H}) \approx 8.3 \pm 0.2$ (Pettini & Pagel 2004). This is consistent with the upper limit of <8.4 found for the host galaxy of FRB 121102 (Tendulkar et al. 2017). The flux line ratios log ([O III] $\lambda5007/$Hβ) ≈ 0.32 and $\log$([N II] $\lambda6583/$Hα) ≈ -1.09 place this galaxy in the star-forming region of the Baldwin, Phillips, and Terlevich (BPT) diagram (Baldwin et al. 1981).

In addition, we obtained narrow-band imaging of ESO 601–G036 with GMOS on Gemini-South on 2018 July 15. We observed for an exposure time of 3 × 180 s using the HaC filter (6590–6650 Å), ensuring full coverage of the Hα emission from this galaxy at redshift $z \sim 0.008$ (Figure 1).

4.2. Radio Continuum Follow-up of ESO 601–G036

To search for a "persistent" radio source, we carried out radio continuum observations using the Australia Telescope Compact Array (ATCA). The initial observations were carried out on 2018 May 27 UT across a wide frequency range to search for a compact radio source in ESO 601−G036 and to compare its spectral energy distribution (SED) with the persistent source of FRB 121102.

Using an extended ATCA array (6D configuration) and Briggs weighting with robust = 0.5 resulted in synthesized beam sizes ranging from $17\farcs4 \times 4\farcs0$ at 2.1 GHz to $1\farcs8 \times 0\farcs3$ at 21.2 GHz. This gives rms noise levels of 40.5, 13.7, 13.2, 21.1, and 31.8 μJy at frequencies of 2.1, 5.5, 9.0, 16.7, and 21.2 GHz, respectively.[12] No radio continuum emission associated with ESO 601−G036 was detected at any frequency.

[12] The rms was calculated from the central 10% of the primary-beam corrected image at each frequency except at 2.1 GHz, where the central 3% was used to avoid nearby sources.

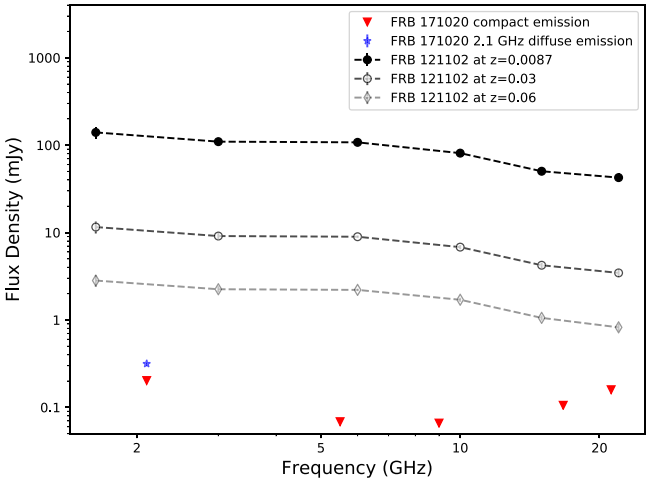

Figure 2. Flux density limits reached from ATCA observations of ESO 601–G036. The red triangles denote 5× rms values. Black points show the flux density of the persistent radio source detected in the repeating FRB if it were observed at $z = 0.0087$ (the redshift of ESO 601–G036), $z = 0.03$ (open circles), and $z = 0.06$ (open diamonds). The blue star shows the integrated flux density of the extended emission detected in deeper 2.1 GHz observations. Error bars are plotted, but are generally smaller than the data points given the large range in flux density shown.

Table 3
Comparison of ESO 601–G036 and the Host Galaxy of the Repeating FRB 121102

	ESO 601–G036	FRB 121102 Host Galaxy
Hubble type	Sc	Dwarf
Redshift	0.008672	0.19273
D_L (Mpc)	37	972
M_R (mag)	−17.9	−17.0
SFR ($M_\odot$ yr^{-1})	0.13	0.23–0.4
Stellar mass ($M_\odot$)	9×10^8	1×10^8
log([N II] λ6583/Hα)	−1.09	⩽−1.34
12 + log([O/H]	8.3 ± 0.2	<8.4
Radio continuum (W Hz^{-1})	$<3.6 \times 10^{19}$	2.3×10^{22}
Host galaxy DM (pc cm^{-3})	∼64–76	55–255

Note. The values quoted for the FRB 121102 host galaxy are from Tendulkar et al. (2017) and Bassa et al. (2017).

Figure 2 shows the 5σ flux density limits reached at each frequency. If ESO 601–G036 hosts this FRB, there is no coincident radio source above a radio luminosity of $L_{2.1\mathrm{GHz}} = 3.6 \times 10^{19}$ W Hz^{-1} (5σ), i.e., 600 times fainter than that seen in the repeating FRB.

Subsequent observations were carried out over the entire localization area at 1–3 GHz using a more compact array configuration (1.5D) on 2018 June 28 UT. The increased sensitivity (rms = 13.0 μJy) and lower resolution of these observations revealed a faint continuum source at the center of ESO 601−G036 with a flux density of $S_{2.1\mathrm{GHz}} = 240$ μJy (with a beam size of 37.″1 × 5.″0). Re-imaging using natural weighting gives a beam size of 83.″8 × 12.″3 and a flux density of $S_{2.1\mathrm{GHz}} = 315$ μJy and indicates that the source is resolved. Using the naturally weighted flux density gives a radio luminosity of $L_{2.1\mathrm{GHz}} = 4.3 \times 10^{19}$ W Hz^{-1}. As this radio detection is resolved we discount it as being similar to the persistent radio source detected in FRB 121102, which is compact on mas-scales. Figure 1 shows the 2.1 GHz data of the field. None of the candidates selected from the WISE × SCOSPZ catalog have associated radio emission (5σ limits are listed in Table 2).

5. Comparison of ESO 601–G036 with the Host Galaxy of FRB 121102

Table 3 compares key properties of ESO 601–G036 with those of the host galaxy of the repeating FRB 121102. $\mathrm{DM_{host}}$ was estimated by assuming that all excess DM is attributed to the host galaxy.

ESO 601–G036 is about a magnitude more luminous than the host galaxy of FRB 121102 (Tendulkar et al. 2017), and the measured projected size of the galaxy (9.2 × 3.7 kpc) is slightly larger. The current star formation rate in ESO 601–G036 is two to three times lower than in the FRB 121102 host, but the two galaxies are qualitatively similar.

The most striking difference is that ESO 601–G036 does not contain a luminous persistent radio source like that seen in the FRB 121102 host galaxy. If ESO 601–G036 is indeed the host galaxy of FRB 171020, this would imply that not all FRBs are associated with bright, compact, and persistent radio emission.

5.1. Searching for FRB 121102 Analogs

As there is no evidence of a compact, persistent radio source associated with ESO 601–G036, we consider whether or not there are other sources in the field that have similar properties to the host galaxy of FRB 121102, but may have been missed by the optical catalogs used in Section 3. In the SuperCOSMOS passbands the host galaxy of FRB 121102 has optical magnitudes $B = 26.2$ and $R = 25.2$, meaning it would be detected above the SuperCOSMOS magnitude limits out to $z = 0.06$. At this redshift, the persistent radio source would be detected above ∼2.5 mJy at 2.1 GHz and be brighter than $S_{2.1\mathrm{GHz}} \sim 10$ mJy if it was at $z < 0.03$.

There are 23 radio sources with $S_{2.1\mathrm{GHz}} > 2.5$ mJy detected in the localization region of FRB 171020, but only seven of these are also detected in SuperCOSMOS. Of these seven radio sources listed in Table 2, two are cataloged in WISE × SCOSPZ with a photometric redshift $z_{\mathrm{ph}} > 0.1$, and three have WISE colors consistent with LIRGs or QSOs, indicating that these are likely background active galactic nuclei (AGN). The remaining two galaxies were observed with X-Shooter but no Hα was detected, indicating that these are at $z > 0.1$ and therefore likely background AGN. As such, we find no sources with similar observed optical and radio properties as the host galaxy of FRB 121102 out to $z = 0.06$.

6. Conclusion

We have searched for a potential host galaxy of FRB 171020 and found ESO 601–G036 to be the most likely candidate given its low redshift and position close to the center of the error ellipse. UV imaging from *GALEX* and follow-up spectroscopic observations reveal that ESO 601–G036 is a low-metallicity galaxy with an SFR of 0.13 $M_\odot$ yr^{-1}, similar to the host galaxy of FRB 121102. However, no compact persistent radio continuum source is detected above

$L_{2.1\mathrm{GHz}} = 3.6 \times 10^{19}\,\mathrm{W\,Hz^{-1}}$, which is 600 times fainter than the persistent source associated with FRB 121102. There is no galaxy within the localization uncertainty region that has similar properties to the host galaxy of FRB 121102 at redshifts $z \lesssim 0.06$. This suggests that not all FRBs have an associated "persistent" radio source. As such, identifying host galaxies based on the presence of a compact, luminous radio continuum source may not necessarily help in identifying host galaxies of FRBs.

The authors wish to thank S. Chatterjee, C. Bassa, and the anonymous referee for useful discussions and suggestions that helped to improve this Letter. This research is based on observations collected at the European Southern Observatory under ESO programme 0101.A-0455(B) (PI: J.-P. Macquart), as well as on observations obtained as part of program GS-2018A-Q-205 (PI: N. Tejos) at the Gemini Observatory and C3211 (PI: R.M. Shannon) on the Australia Telescope Compact Array. J.P.M., R.M.S., and K.B. acknowledge Australian Research Council grant DP180100857 and R.M.S. acknowledges support through Australian Research Council (ARC) grants FL150100148 and CE17010000.

The Australian SKA Pathfinder is part of the Australia Telescope National Facility which is managed by CSIRO. We acknowledge the Wajarri Yamatji as the traditional owners of the Observatory site. The Australia Telescope Compact Array is part of the Australia Telescope National Facility which is funded by the Australian Government for operation as a National Facility managed by CSIRO. The Gemini Observatory is operated by the Association of Universities for Research in Astronomy, Inc., under a cooperative agreement with the NSF on behalf of the Gemini partnership: the National Science Foundation (United States), the National Research Council (Canada), CONICYT (Chile), Ministerio de Ciencia, Tecnología e Innovación Productiva (Argentina), and Ministério da Ciência, Tecnologia e Inovação (Brazil).

Facilities: ASKAP, ATCA, *WISE*, VISTA, *GALEX*, Gemini-S, VLT.

Software: astropy (Astropy Collaboration et al. 2013), PyRAF.

ORCID iDs

Elizabeth K. Mahony https://orcid.org/0000-0002-5053-2828
Ron D. Ekers https://orcid.org/0000-0002-3532-9928
Jean-Pierre Macquart https://orcid.org/0000-0001-6763-8234
Keith W. Bannister https://orcid.org/0000-0003-2149-0363
Chris Flynn https://orcid.org/0000-0002-4796-745X
J. Xavier Prochaska https://orcid.org/0000-0002-7738-6875
Stuart D. Ryder https://orcid.org/0000-0003-4501-8100
O. I. Wong https://orcid.org/0000-0002-2504-7628

References

Astropy Collaboration, Robitaille, T. P., Tollerud, E. J., et al. 2013, A&A, 558, A33
Baldwin, J. A., Phillips, M. M., & Terlevich, R. 1981, PASP, 93, 5
Bannister, K. W., Shannon, R. M., Macquart, J. P., et al. 2017, ApJ, 841, L12
Barnes, D. G., Staveley-Smith, L., de Blok, W. J. G., et al. 2001, MNRAS, 322, 486
Bassa, C. G., Tendulkar, S. P., Adams, E. A. K., et al. 2017, ApJL, 843, L8
Bhandari, S., Keane, E. F., Barr, E. D., et al. 2018, MNRAS, 475, 1427
Bilicki, M., Peacock, J. A., Jarrett, T. H., et al. 2016, ApJS, 225, 5
Caleb, M., Keane, E. F., van Straten, W., et al. 2018, MNRAS, 478, 2046
Chatterjee, S., Law, C. J., Wharton, R. S., et al. 2017, Natur, 541, 58
Cordes, J. M., & Lazio, T. J. W. 2002, arXiv:astro-ph/0207156
da Costa, L. N., Willmer, C. N. A., Pellegrini, P. S., et al. 1998, AJ, 116, 1
Dolag, K., Gaensler, B. M., Beck, A. M., & Beck, M. C. 2015, MNRAS, 451, 4277
Eftekhari, T., & Berger, E. 2017, ApJ, 849, 162
Eftekhari, T., Berger, E., Williams, P. K. G., & Blanchard, P. K. 2018, ApJ, 860, 73
Gimeno, G., Roth, K., Chiboucas, K., et al. 2016, Proc. SPIE, 9908, 99082S
Hook, I. M., Jørgensen, I., Allington-Smith, J. R., et al. 2004, PASP, 116, 425
Inoue, S. 2004, MNRAS, 348, 999
Ioka, K. 2003, ApJL, 598, L79
Irwin, M. J., Lewis, J., Hodgkin, S., et al. 2004, Proc. SPIE, 5493, 411
Jones, D. H., Saunders, W., Colless, M., et al. 2004, MNRAS, 355, 747
Kopparapu, R. K., Hanna, C., Kalogera, V., et al. 2008, ApJ, 675, 1459
Lauberts, A. 1982, ESO/Uppsala Survey of the ESO(B) Atlas (Garching: ESO)
Manchester, R. N., Hobbs, G. B., Teoh, A., & Hobbs, M. 2005, AJ, 129, 1993
Marcote, B., Paragi, Z., Hessels, J. W. T., et al. 2017, ApJL, 834, L8
Masui, K., Lin, H.-H., Sievers, J., et al. 2015, Natur, 528, 523
McQuinn, M. 2014, ApJL, 780, L33
Meyer, M. J., Zwaan, M. A., Webster, R. L., et al. 2004, MNRAS, 350, 1195
Michilli, D., Seymour, A., Hessels, J. W. T., et al. 2018, Natur, 553, 182
Miller, M. J., & Bregman, J. N. 2013, ApJ, 770, 118
Mould, J. R., Huchra, J. P., Freedman, W. L., et al. 2000, ApJ, 529, 786
Petroff, E., Barr, E. D., Jameson, A., et al. 2016, PASA, 33, e045
Petroff, E., Burke-Spolaor, S., Keane, E. F., et al. 2017, MNRAS, 469, 4465
Pettini, M., & Pagel, B. E. J. 2004, MNRAS, 348, L59
Planck Collaboration, Ade, P. A. R., Aghanim, N., et al. 2016, A&A, 594, A13
Shannon, R. M., Macquart, J.-P., Bannister, K. W., et al. 2018, Natur, 562, 386
Spitler, L. G., Scholz, P., Hessels, J. W. T., et al. 2016, Natur, 531, 202
Tendulkar, S. P., Bassa, C. G., Cordes, J. M., et al. 2017, ApJL, 834, L7
Vernet, J., Dekker, H., D'Odorico, S., et al. 2011, A&A, 536, A105
Walker, C. R. H., Ma, Y.-Z., & Breton, R. P. 2018, arXiv:1804.01548
Wong, O. I., Meurer, G. R., Zheng, Z., et al. 2016, MNRAS, 460, 1106
Xu, J., & Han, J. L. 2015, RAA, 15, 1629
Yao, J. M., Manchester, R. N., & Wang, N. 2017, ApJ, 835, 29